R. & M. No. 2842
(14,334)
(A.R.C. Technical Report)

Copy B

MINISTRY OF SUPPLY

AERONAUTICAL RESEARCH COUNCIL
REPORTS AND MEMORANDA

The Theoretical Wave Drag of Some Bodies of Revolution

By

L. E. FRAENKEL

LONDON: HER MAJESTY'S STATIONERY OFFICE
1955
SEVEN SHILLINGS NET

The Theoretical Wave Drag of Some Bodies of Revolution

By

L. E. FRAENKEL

COMMUNICATED BY THE PRINCIPAL DIRECTOR OF SCIENTIFIC RESEARCH (AIR), MINISTRY OF SUPPLY

Reports and Memoranda No. 2842*

May, 1951

Summary.—This report investigates the wave drag of bodies of revolution with pointed or open-nose forebodies and pointed or truncated afterbodies. The 'quasi-cylinder' and 'slender-body' theories are reviewed, a reversibility theorem is established, and the concept of the interference effect of a forebody on an afterbody is introduced.

The theories are applied to bodies whose profiles are either straight or parabolic arcs, formulae and curves being given for forebody and afterbody drag, and for the interference drag. The results of the two theories are compared and are seen to agree well in the region of geometries where both theories are applicable.

1. *Introduction.*—The solution of the linearised equation for the supersonic flow past bodies of revolution, originally due to von Kármán[1], has in recent years been extended by Lighthill[2,3] and Ward[4] to cover a considerable variety of shapes. In particular these authors have made possible direct calculation of the lift and drag of open-nose bodies, the flow about which differs fundamentally from that about a pointed body in that the flow at the open end is of a two-dimensional nature. Two different types of approximation have been developed; the 'quasi-cylinder' solution, which assumes that the radius of the body departs only slightly from some mean, and the 'slender-body' solution, which assumes that the maximum diameter of the body is small relative to its length.

The present paper is concerned only with the wave drag of bodies at zero incidence, and is an application of Lighthill's theory to some particular cases. The work is simplified by dividing the drag into the components shown below, and by a reversibility theorem which follows directly from Refs. 2 and 3.

If we consider a body consisting of a forebody, a parallel mid-portion, and an afterbody, the total drag is the sum of the following three components:

(*a*) The forebody drag

(*b*) The 'principal afterbody drag,' which is the drag that the afterbody would have if it were situated behind an infinitely long parallel portion

(*c*) The interference drag due to the effect of the forebody on the afterbody.

---

* R.A.E. Report Aero. 2420, received 29th October, 1951.

A

It will be shown that, to the order of accuracy of the theory used, the drag of a body is equal to that of its 'reverse'; and therefore forebody drag and principal afterbody drag, which depend only on the shape of the profile in question, are equal if the shapes are the reverse of one another. Further, the 'interference pressure' at any point on an afterbody depends only on the shape of the forebody and on the axial distance of the point behind it. The interference drag decays rapidly as the length of the parallel position is increased; when this length is of the order of the forebody length, the interference effect is negligible.

The notation used in this report, which differs slightly from that of the original papers, is given after Appendix I and is shown in Fig. 1.

Where equations are quoted from the original papers the numbers in square brackets indicate, respectively, the reference number of the paper from which an equation is taken and the number of the corresponding equation in that paper.

2. *Summary of the Work of Lighthill.*—2.1. *The Quasi-cylinder Theory.*—In Ref. 2 the pressure coefficient at any external point of a quasi-cylinder of mean radius R is found to be

$$C_p = \frac{2}{B}\int_{s=0-}^{z} U(z-s)\, d\eta(s), \qquad (1)\ [2.79]$$

where the integral is taken in the Stieltjes sense*, and $B = \sqrt{(M^2-1)}$, $z = x/BR$, $\eta(z) = dr/dx$, the slope of the body profile at any point.

$U(z)$ is a function derived by Lighthill, and is tabulated in Ref. 2 for $z = 0$ to 10. Some idea of its behaviour is given by the properties

$$\begin{aligned} U(z) &= 0 \text{ for } z < 0, \\ &= 1 \text{ for } z = 0, \\ &\sim \frac{1}{z} \text{ for } z \text{ large.} \end{aligned}$$

$U(z)$ and some associated functions, which are necessary for the work of the present paper, are tabulated for $z = 0$ to 20 in Table 1, and are discussed more fully in Appendix I.

Writing $\quad U'(x) = -W(x)$,

where the dash denotes differentiation, and applying integration by parts to (1), one obtains

$$C_p = \frac{2}{B}\left[\eta(z) - \int_0^z W(z-s)\,\eta(s)\,ds\right]. \qquad (1a)\ [2.83]$$

(1) and (1a) are valid for profiles having discontinuities in slope, the change in pressure at a discontinuity being the two-dimensional value

$$\Delta C_p = \frac{2}{B}\Delta\eta. \qquad (2)$$

To the order of approximation of the theory the drag is given by

$$\frac{D}{\frac{1}{2}\rho V^2} = \int_0^c C_p . 2\pi R\eta(z) . BR\, dz, \qquad (3)$$

where cBR is the length of the body; substituting (1a) into (3) gives

$$C_D = \frac{R^2}{R_{\max}^{\ 2}}\left[4\int_0^c \eta^2(z)\,dz - 2\int_0^c\int_0^c W(|z-s|)\,\eta(z)\,\eta(s)\,dz\,ds\right]. \qquad (4)\ [2.84]$$

* When dealing with functions having discontinuities in an interval of integration, we shall be careful in this paper to write Stieltjes integrals in the form $\int_{x=a}^{b} f(x)\,dg(x)$. By expressions of the form $\int_a^b f(x)\,g'(x)\,dx$ we shall mean the sum of Riemann integrals taken between the points of discontinuity.

2.2. *The Slender Body Theory.*—In Ref. 2 Lighthill also deals with bodies having a pointed nose, continuous profile slope, and a maximum thickness t. The length of the body is considered to be $O(1)$. If the radius of such a body is $R(x)$, and $S(x)$ is the cross-section area, then the pressure coefficient at any point on the body is*

$$C_p = \frac{1}{\pi}\int_0^{x-BR(x)} \frac{S''(y)}{\sqrt{[(x-y)^2 - B^2R^2(x)]}}\,dy - R'^2(x) + O(t^4 \log^2 t). \qquad (5) \quad [2.26]$$

The integral in (5) may be considered to be due to a distribution of supersonic sources at points y on the x-axis, of strength $S'(y)/2\pi$. An equivalent form is

$$C_p = \frac{1}{\pi}\left[S''(0)\log x + S''(x)\log\frac{2}{BR(x)} + \int_{y=0+}^{x} \log(x-y)\,dS''(y)\right] - R'^2(x)$$

$$+ O(t^4 \log^2 t), \qquad [2.30]$$

$$= \frac{1}{\pi}\int_{y=0-}^{x} \log\frac{2(x-y)}{BR(x)}\,dS''(y) - R'^2(x) + O(t^4 \log^2 t). \qquad (6) \quad [3.29]$$

(6) is not correct in small regions immediately downstream of any discontinuities in $S''(x)$. In fact if such a discontinuity occurs at $x = a$, the change in (5) only becomes effective at $x \simeq a + BR(a)$ and the alternative form (6) gives a logarithmic singularity at $x = a$. Neither of these are physically probable, but their effects are confined to regions of length $O(t)$; and it may be shown that in the drag integral

$$\frac{D}{\frac{1}{2}\rho V^2} = \int_0^l C_p . S'(x)\,dx \qquad (7)$$

the error will still be of $O(t^6 \log^2 t)$. In Ref. 2 Lighthill integrated (6) for bodies having a pointed nose, $[S'(0) = 0]$, and either zero profile slope or a pointed tip at the rear $[S'(l) = 2\pi R(l)R'(l) = 0]$, giving

$$\frac{D}{\frac{1}{2}\rho V^2} = \frac{1}{2\pi}\int_0^l\int_0^l \log\frac{1}{|x-y|}\,S''(x)\,S''(y)\,dx\,dy + O(t^6 \log^2 t). \qquad (8) \quad [2.36]$$

However, only the condition $S'(0) = 0$ and continuity of profile slope are necessary for the application of (6), so that for a body having a truncated afterbody we obtain

$$\frac{D}{\frac{1}{2}\rho V^2} = \frac{1}{2\pi}\int_0^l\int_0^l \log\frac{1}{|x-y|}\,S''(x)\,S''(y)\,dx\,dy - \frac{S'(l)}{\pi}\int_0^l S''(x)\log\frac{1}{l-x}\,dx$$

$$+ \frac{1}{2\pi}S'^2(l)\log\frac{2}{BR(l)} + O(t^6 \log^2 t). \qquad (9)$$

It may be noted in passing that the condition $S'(0) = 0$ is satisfied by afterbodies situated behind a long parallel portion, and whose initial slope is zero. Hence the above results can be applied to such bodies.

In Ref. 3 Lighthill has extended his work to slender bodies with discontinuities in profile slope. He considers a body whose profile extends from $x = a_0$ to a_n and is defined by $r = R(x)$. $R(x)$ is continuous in $a_0 < x < a_n$ and analytic in each of the intervals $a_0 < x < a_1$, $a_1 < x < a_2, \ldots,$ $a_{n-1} < x < a_n$. The change in slope at the points of discontinuity is given by b_i, i.e.,

$$b_i = R'(a_i +) - R'(a_i -),$$

and this is interpreted for $i = 0$ and $i = n$ by specifying that $R'(x) = 0$ for $x < a_0$ and $x > a_n$. $R(a_i)$ is written as R_i.

* The order terms here are based on the work of Ward[7] and of the present author[8] and are not always exactly those given in Refs. 2 and 3.

Approximating as above, Lighthill has shown that the pressure coefficient at any point on the body is

$$C_p = \frac{1}{\pi}\int_{a_0}^{x - BR(x)} \frac{S''(y)\,dy}{\sqrt{[(x-y)^2 - B^2R^2(x)]}} - R'^2(x) + \sum_{i=0}^{n} \frac{2b_i}{B}\, U\left(\frac{x-a_i}{BR_i}\right), \qquad \begin{matrix}(10)\\ [3.23]\end{matrix}$$

where U is the function introduced in 2.1 above. In regions of length $O(t)$ immediately behind the discontinuities the error is $O(t^2)$ because the U-term only gives the two-dimensional pressure change to first order. As in (5) one may replace the integral in (10) by

$$\frac{1}{\pi}\int_{y=a_0-}^{x} \log\frac{2(x-y)}{BR(x)}\, dS''(y). \quad \ldots \qquad \begin{matrix}(11)\\ [3.29]\end{matrix}$$

If $$U_1(x) = \int_0^x U(t)\,dt, \quad [U_1(0) = 0], \quad \ldots \qquad (12)$$

the contribution to the drag integral (7) of the third term in (10) is the sum of terms like

$$\frac{2b_i}{B}\int_{a_i}^{a_n} U\left(\frac{x-a_i}{BR_i}\right) S'(x)\,dx = -\,2b_iR_i\int_{x=a_i+}^{a_n+} U_1\left(\frac{x-a_i}{BR_i}\right) dS'(x). \quad \ldots \qquad \begin{matrix}(13)\\ [3.27]\end{matrix}$$

Hence integrating (10), and using (11) and (13), we eventually obtain

$$\frac{D}{\frac{1}{2}\rho V^2} = \frac{1}{2\pi}\int_{a_0}^{a_n}\int_{a_0}^{a_n} S''(x)\,S''(y)\log\frac{1}{|x-y|}\,dx\,dy$$

$$-\frac{1}{2\pi}\sum_{i=0}^{n}\log\frac{2}{BR_i}\,[S'^2(a_i+) - S'^2(a_i-)]$$

$$+\sum_{i=0}^{n} 2b_iR_i\left[\int_{a_0}^{a_i} S''(x)\log\frac{1}{a_i - x}\,dx - \int_{a_i}^{a_n} S''(x)\,U_1\left(\frac{x-a_i}{BR_i}\right)dx\right]$$

$$-\sum_{i=0}^{n}\sum_{j=i+1}^{n} 4\pi b_ib_jR_iR_j\,.\,U_1\left(\frac{a_j-a_i}{BR_i}\right) + O(t^5). \quad \ldots \qquad (14)$$

A further approximation is possible. The asymptotic expansion of $U_1(x)$ is (Appendix I),

$$U_1(x) \sim \log 2x + O(x^{-2}\log x), \quad \ldots \qquad [3.7]$$

so that one may write $|U_1(x) - \log 2x| < A_0x^{-2}\log x$ for $x > A_1$, say, and for $x < A_1$ we have $U_1(x) < A_2$, say. Hence if we replace $U_1[(x-a_i)/BR_i]$ by $\log[2(x-a_i)/BR_i]$ in the fourth term of (14), the error will be at most the sum of terms like

$$2b_iR_i\int_{a_i+A_1BR_i}^{a_n} |S''(x)|\,.\,A_0\left(\frac{BR_i}{x-a_i}\right)^2\log\frac{x-a_i}{BR_i}\,dx$$

$$+\,2b_iR_i\int_{a_i}^{a_i+A_1BR_i} |S''(x)|\left[A_2 + \left|\log\frac{2(x-a_i)}{BR_i}\right|\right]dx.$$

This expression is $O(t^5)$, and (14) therefore becomes

$$\frac{D}{\frac{1}{2}\rho V^2} = \frac{1}{2\pi}\int_{a_0}^{a_n}\int_{a_0}^{a_n} S''(x)\, S''(y) \log \frac{1}{|x-y|}\, dx\, dy$$

$$-\frac{1}{2\pi}\sum_{i=0}^{n} \log \frac{2}{BR_i}\,[S'^2(a_i+) - S'^2(a_i-)]$$

$$+\sum_{i=0}^{n} 2b_iR_i \int_{a_0}^{a_n} S''(x) \log \frac{1}{|x-a_i|}\, dx$$

$$-\sum_{i=0}^{n} 2b_iR_i \log \frac{2}{BR_i} \sum_{j=i+1}^{j=n} [-S'(a_{j-1}+) + S'(a_j-)]$$

$$-\sum_{i=0}^{n}\sum_{j=i+1}^{n} 4\pi b_ib_jR_iR_j\,.\, U_1\left(\frac{a_j-a_i}{BR_i}\right) + O(t^5). \quad \ldots \qquad (15)$$

In the last term of (15) we may write

$$U_1\left(\frac{a_j-a_i}{BR_i}\right) \simeq \log \frac{2(a_j-a_i)}{BR_i} \quad \ldots \qquad (16)$$

and the error will be $O(t^6 \log t)$, *provided that* the distance between the discontinuities concerned is large with respect to the thickness of the body. This restriction becomes important when we consider a forebody and an afterbody joined by a parallel portion, and let the length of the parallel portion tend to zero.

If the discontinuities are all spaced well apart, we may use (16), and (15) becomes

$$\frac{D}{\frac{1}{2}\rho V^2} = \frac{1}{2\pi}\int_{a_0}^{a_n}\int_{a_0}^{a_n} S''(x)\, S''(y) \log \frac{1}{|x-y|}\, dx\, dy$$

$$+\sum_{i=0}^{n} 2b_iR_i \int_{a_0}^{a_n} S''(x) \log \frac{1}{|x-a_i|}\, dx$$

$$+\sum_{i=0}^{n}\sum_{j=i+1}^{n} 4\pi b_ib_jR_iR_j \log \frac{1}{a_j-a_i}$$

$$+\sum_{i=0}^{n} 2\pi b_i^2R_i^2 \log \frac{2}{BR_i} + O(t^5). \quad \ldots \qquad (17)$$

[3.35 and 3.36]

As is shown in Ref. 3, this may be written

$$\frac{D}{\frac{1}{2}\rho V^2} = \frac{1^*}{2\pi}\int_{x=a_0-}^{a_n+}\int_{y=a_0-}^{a_n+} \log \frac{1}{|x-y|}\, dS'(x)\, dS'(y)$$

$$+\sum_{i=0}^{n} 2\pi b_i^2R_i^2 \log \frac{2}{BR_i} + O(t^5) \quad \ldots \qquad (17a)$$

[3.38]

where the asterisk denotes the ' finite part of ' the Stieltjes integral.

If we put $b_1 = b_2 = \ldots = b_{n-1} = 0$, and either b_0 or $R_0 = 0$, (17) reduces to (9).

3. *Further Results of the Theories.*—3.1. *Reversibility Theorem.*—The drag of a quasi-cylinder is given by (4). We write $z = c - Z$ and $s = c - S$, and (4) becomes

$$C_D = \frac{R_{max}^2}{R^2}\left[4\int_0^c \eta^2(c-Z)\,dZ \quad - 2\int_0^c\int_0^c W(|Z-S|)\eta(c-Z)\,\eta(c-S)\,dZ\,dS\right]. \qquad (18)$$

But the 'reverse' of the body, which we denote by subscript r, is defined by

$$\eta_r(Z) = -\,\eta(c-Z) \text{ and } R_r = R,$$

so that we may write (18)

$$C_D = \frac{R_r^2}{R_{max}^2}\left[4\int_0^c \eta_r^2(Z)\,dZ - 2\int_0^c\int_0^c W(|Z-S|)\,\eta_r(Z)\eta_r(S)\,dZ\,dS\right]. \quad .. \qquad (19)$$

Hence a quasi-cylinder and its reverse have the same drag. The reversibility of slender bodies with all discontinuities spaced well apart may be shown similarly from (17) or (17a). If the distance between certain pairs of discontinuities, denoted by $x = a_m$ and a_{m+1}, is $O(t)$, (17) is no longer applicable, but the reversibility theorem still holds. In this case the drag may be written as the reversible form (17) plus

$$\Sigma 4\pi b_m b_{m+1} R_m R_{m+1}\left[\log\frac{2(a_{m+1}-a_m)}{BR_m} - U_1\left(\frac{a_{m+1}-a_m}{BR_m}\right)\right], \quad .. \qquad (20)$$

where the summation refers to the different pairs of discontinuities close to each other. Clearly these terms are reversible if $R_m = R_{m+1}$, which is the case if a_m and a_{m+1} denote the end points of a parallel portion. If $R_m \neq R_{m+1}$, we have

$$\begin{aligned} R_{m+1} &= R_m + (a_{m+1} - a_m)R'(a_m) + \ldots \\ &= R_m + O(t^2), \end{aligned}$$

and the difference between (20) and the equivalent terms for the reversed body will be $O(t^5)$, and therefore negligible.

3.2. *The Two Components of Afterbody Drag.*—Consider a quasi-cylinder with forebody extending from $z = 0$ to a, a parallel portion from a to b, and an afterbody from b to c. We denote the fore- and afterbody by subscripts F and A respectively. Then by (1) the pressure coefficient at any point on the afterbody may be written

$$C_{p\,A} = C_{p\,A1} + C_{p\,A2},$$

where $$C_{p\,A1} = \frac{2}{B}\int_{s=b-}^{z} U(z-s)\,d\eta_A(s), \quad .. \quad .. \quad .. \quad .. \quad .. \quad .. \qquad (21)$$

and $$\begin{aligned} C_{p\,A2} &= \frac{2}{B}\int_{s=0-}^{a+} U(z-s)\,d\eta_F(s) \\ &= -\frac{2}{B}\int_0^a W(z-s)\,\eta_F(s)\,ds. \quad .. \quad .. \quad .. \quad .. \quad .. \quad .. \end{aligned} \qquad (22)$$

$C_{p\,A1}$ is the pressure coefficient associated with the afterbody profile alone (*i.e.*, if it were situated behind a long parallel portion); we call the integral of $C_{p\,A1}$ over the afterbody the principal afterbody drag, $C_{D\,A1}$. $C_{p\,A2}$ gives the interference effect of the forebody; (22) shows that this depends only on the forebody shape and the distance of the point z behind it. Also, in view of the asymptotic expansion of $U(z)$, $C_{p\,A2} \to 0$ as $z \to \infty$; this decay is quite rapid.

The principal afterbody drag is an integral like (4) ; the interference drag may be written

$$C_{D'A2} = -\frac{4R^2}{R_{\max}{}^2}\int_b^c \eta_A(z)dz\int_0^a W(z-s)\,\eta_F(s)\,ds. \quad \ldots \quad (23)$$

A similar procedure can be applied to slender bodies. Let the parallel portion of such a body extend from $x = a_k$ to a_{k+1}. Then from (10) and (11) we have

$$C_{p\,A1} = \frac{1}{\pi}\int_{y=a_{k+1}-}^{x} \log\frac{2(x-y)}{BR(x)}\,dS''(y) - R'^2(x) + \sum_{i=k+1}^{n}\frac{2b_i}{B}\,U\left(\frac{x-a_i}{BR_i}\right), \quad \ldots \quad (24)$$

$$C_{p\,A2} = \frac{1}{\pi}\int_{y=a_0-}^{a_k+} \log\frac{2(x-y)}{BR(x)}\,dS''(y) + \sum_{i=0}^{k}\frac{2b_i}{B}\,U\left(\frac{x-a_i}{BR_i}\right)$$

$$= \frac{1}{\pi}\int_{a_0}^{a_k}\frac{S''(y)}{x-y}\,dy + \sum_{i=0}^{k}\frac{2b_i}{B}\,U\left(\frac{x-a_i}{BR_i}\right). \quad \ldots \quad (25)$$

$C_{p\,A1}$ and $C_{p\,A2}$ obviously have the same characteristics here as were mentioned above for the quasi-cylinder case. The interference drag is

$$\frac{D_{A\,2}}{\frac{1}{2}\rho V^2} = \frac{1}{\pi}\int_{a_{k+1}}^{a_n} S'(x)\,dx\int_{a_0}^{a_k}\frac{S''(y)}{x-y}\,dy - \sum_{i=0}^{k} 2b_iR_i\int_{a_{k+1}-}^{a_n} U_1\left(\frac{x-a_i}{BR_i}\right)dS'(x)$$

$$= \frac{1}{\pi}\int_{a_{k+1}}^{a_n} S'(x)\,dx\int_{a_0}^{a_k}\frac{S''(y)}{(x-y)}\,dy - \sum_{i=0}^{k} 2b_iR_i\int_{a_{k+1}}^{a_n}\log\frac{2(x-a_i)}{BR_i}\,S''(x)\,dx$$

$$- \sum_{i=0}^{k}\sum_{j=k+1}^{n} 4\pi b_ib_jR_iR_jU_1\left(\frac{a_j-a_i}{BR_i}\right). \quad \ldots \quad (26)$$

In general the interference drag is appreciable only when the parallel portion is short, so that we shall not want to make the substitution

$$U_1\left(\frac{a_{k+1}-a_k}{BR_k}\right) \simeq \log\frac{2(a_{k+1}-a_k)}{BR_k}.$$

However, if $a_{k+1} - a_k >> BR_k$, the expression for $D_{A\,2}$ similar to (17) is

$$\frac{D_{A\,2}}{\frac{1}{2}\rho V^2} = \frac{1}{\pi}\int_{a_0}^{a_k} S''(y)\,dy\int_{a_{k+1}}^{a_n} S''(x)\log\frac{1}{x-y}\,dx$$

$$+ \sum_{i=0}^{k} 2b_iR_i\int_{a_{k+1}}^{a_n} S''(x)\log\frac{1}{x-a_i}\,dx$$

$$+ \sum_{i=k+1}^{n} 2b_iR_i\int_{a_0}^{a_k} S''(x)\log\frac{1}{a_i-x}\,dx$$

$$+ \sum_{i=0}^{k}\sum_{j=k+1}^{n} 4\pi b_ib_jR_iR_j\log\frac{1}{a_j-a_i}. \quad \ldots \quad (27)$$

It may be noted that this is independent of Mach number.

4. *Applications*.—4.1. *General*.—Most of the following work is based on the slender-body theory, because comparison of the two approximations (section 4.4 and Figs. 9 and 10) shows that for area ratios $S_0/S_{\max} > 0 \cdot 6$—that is, in the region of geometries where we may have considerable confidence in the quasi-cylinder theory—the slender-body theory gives good agreement with the quasi-cylinder theory even for bodies whose fineness ratio is so low that the use of the slender body theory can no longer be rigorously justified. On the other hand the quasi-cylinder theory does not give good agreement for slender bodies of small area ratio.

We have of course no justification for either approximation in the region where the fineness ratio and the area ratio are both of low value. However, as Lighthill has pointed out in Ref. 3, the slope of profiles in this region is too great to permit use of the linearised equation, so that there is little to be gained by solving this equation exactly (which can be done by the numerical solution of an integral equation). In fact it may be shown that the difference between the slender body solution and the exact solution of the linearised equation is, mathematically, of the same order as the error which results in either case from neglecting higher-order terms of the exact equation.

Thus it may be argued that the drag of all bodies to which the linearised equation is applicable—that is, bodies whose profile slope is reasonably small—may be calculated adequately by the slender-body theory. Nevertheless the quasi-cylinder theory should not be dismissed entirely, because for bodies with area ratios $> 0 \cdot 6$ it has the following advantages: (*a*) It gives a pressure distribution which is more realistic than that of the slender-body theory in the vicinity of points of discontinuity of $S''(x)$; and (*b*), the algebra involved in the use of the quasi-cylinder theory is in general less cumbersome.

The effect of Mach number on the validity of the theories should also be mentioned. In the derivation of the theories $\sqrt{(M^2 - 1)}$ is assumed to be $O(1)$: in practice a lower limit to the Mach number range may be provided by the requirement that the flow be supersonic everywhere, and an upper limit by the requirement that the product of $\sqrt{(M^2 - 1)}$ and profile slope be small. Thus, as far as the upper limit is concerned, 'fineness ratio' in the discussion above may be interpreted to mean the parameter $l/R\sqrt{(M^2 - 1)}$ which appears in the figures.

If it is required to find the pressure distribution on a given body to a greater accuracy than that of the approximations given here, this can often be done quite simply by fairing the curves given by the approximate theories into known exact values at certain points. For example at the nose of a pointed body, or at a discontinuity in slope or in curvature, the exact pressure changes can easily be computed, and it is just at these points that the approximate theories tend to be seriously in error. Such a procedure has not been followed in this report because the simplicity of the drag formulae would be lost, so that a limited amount of calculation would no longer yield anything like the same number of results. Even the calculation of pressure distributions as given by the above theory for the range of geometries and Mach numbers considered here would require very much more labour than is required to find the drag coefficients.

Only results are quoted in the sections below because the integrations which lead to them are straightforward in all cases. We define the fineness ratio of a forebody, afterbody or parallel portion as length/maximum radius, and that of a complete body as length/maximum diameter, in order that the two halves of a symmetrical body may have the same fineness ratio as the complete body. In the expressions for drag the shape of a forebody or afterbody is described by the nature of its profile, its fineness ratio, and the ratio of the length of the body to the length of the corresponding pointed body (*i.e.*, the same body continued to a point at the smaller end). In the figures, however, this last ratio has been replaced by an area ratio, which was thought to be more convenient from the practical point of view.

4.2. *Bodies of Parabolic Profile.*—It may be mentioned in passing that the difference between a parabola (near its vertex) and a circular-arc is small. If we consider two bodies of equal overall dimensions and of thickness ratio t, one having a parabolic and the other a circular-arc profile, the difference in radius and slope at any other point is $O(t^3)$, and it may be shown that the difference in drag is $O(t^6 \log t)$. Since slender-body theory only gives drag correct to $O(t^5) = 0$, the difference between the two profiles is negligible, and the results derived below for parabolic profiles may also be used for circular-arc profiles, (ogives).

Fig. 2 shows, as an example, the pressure distribution about a symmetrical, pointed body of parabolic profile. The length of the body is 1 and the maximum diameter t; hence

$$R(x) = 2t(x - x^2). \qquad (28)$$

(5) and (6) become, respectively,

$$\frac{C_p}{4t^2} = 2[1 - 6x + (6 + 12B^2t^2)x^2 - 24B^2t^2x^3 + 12B^2t^2x^4] \cosh^{-1} \frac{1}{2Bt(1 - x)}$$
$$+ 6(2x - 3x^2)\sqrt{(1 - 4B^2t^2 + 8B^2t^2x - 4B^2t^2x^2)} - (1 - 2x)^2, \qquad (29)$$

and

$$\frac{C_p}{4t^2} = 2(1 - 6x + 6x^2) \log \frac{1}{Bt(1 - x)} - 1 + 16x - 22x^2. \qquad (30)$$

The two forms are virtually coincident for the case $Bt = 0 \cdot 1$; for $Bt = 0 \cdot 4$ the difference is appreciable but its effect upon the drag would not appear to be large, and the error due to the logarithmic form is conservative.

The (principal) drag of a parabolic forebody (or afterbody) is, from (9) or (17),

$$C_D \,.\, a^2 = \frac{4}{b^8}\left[2(b^2 - 1)^2 \log \frac{2\beta b^2}{b^2 - 1} - \tfrac{10}{3} + \tfrac{11}{2}b^2 - b^4 \right] \qquad (31)$$

where a and ab are the fineness ratios of the body and of the corresponding pointed body, respectively, and $\beta = a/B$. For pointed bodies ($b = 1$) the drag coefficient is independent of Mach number and is

$$C_D \,.\, a^2 = 14/3. \qquad (32)$$

Equation (31) is plotted in Fig. 3, the ratio b being replaced by an area ratio (which depends on b only). The portions of the curves which cover low values of both the area ratio S_0/S_1 and the parameter $l/R_1\sqrt{(M^2 - 1)}$ correspond to regions where there is no justification for the theory and are shewn chain-dotted. Such a separation of 'acceptable' from 'unacceptable' values is of course rather arbitrary; the criterion used here is that for the acceptable values

$$\text{(maximum profile slope)}. \sqrt{(M^2 - 1)} \leqslant 1/5.$$

A limited number of comparisons with exact theory and with experiment indicates that at the boundary of the two regions the theory is in error by about 10 per cent for forebodies and 15 per cent for afterbodies.

For pointed bodies consisting of two parabolic parts and a parallel portion the drag is the sum of two terms like (32) and the interference drag. (26) or (27) give the interference drag as

$$C_{D\,A2} \,.\, a^2 = \frac{4}{c^4} \{[(-1 + c^2 + c^4 - c^6) - \tfrac{16}{5}(1 + c^5)p - (3 + 2c^2 + 3c^4)p^2 + (1 + c^2)p^4 - \tfrac{1}{5}p^6] \log (1 + c + p)$$
$$+ [(-c^4 + c^6) + \tfrac{16}{5}c^5p + (2c^2 + 3c^4)p^2 - (1 + c^2)p^4 + \tfrac{1}{5}p^6] \log (c + p)$$
$$+ [(1 - c^2) + \tfrac{16}{5}p + (3 + 2c^2)p^2 - (1 + c^2)p^4 + \tfrac{1}{5}p^6] \log (1 + p)$$
$$+ [-2c^2p^2 + (1 + c^2)p^4 - \tfrac{1}{5}p^6] \log p$$
$$+ (c - \tfrac{1}{2}c^2 - \tfrac{2}{3}c^3 - \tfrac{1}{2}c^4 + c^5) + \tfrac{1}{5}(11c - 3c^2 - 3c^3 + 11c^4)p$$
$$+ \tfrac{2}{5}(2c - \tfrac{3}{4}c^2 + 2c^3)p^2 + \tfrac{1}{5}(c + c^2)p^3 - \tfrac{1}{5}cp^4\}, \qquad (33)$$

where a, ap, and ac are the fineness ratios of the afterbody, parallel portion, and forebody respectively. (33) is plotted in Fig. 4. When the parallel portion is as long as the forebody or longer, the interference drag is less than 3 per cent of the total body drag.

For a body having a pointed forebody, a truncated afterbody and no parallel portion, the interference drag is

$$C_{D\,A2} \,.\, a^2 = \frac{4}{b^4c^4}\{[(2-3b^2)-(1-2b^2)c^2+b^2c^4-c^6]\log(1+c)-(b^2-c^2)c^4\log c$$
$$-(2-3b^2)c+(1-\tfrac{3}{2}b^2)c^2+(\tfrac{1}{3}-b^2)c^3-\tfrac{1}{2}c^4+c^5\}, \quad \ldots \quad (34)$$

where a, ab and ac are the fineness ratios of the afterbody, the pointed equivalent of the afterbody, and the forebody, respectively. Equation (34) is plotted in Fig. 5.

In Fig. 6 equations (31), (32) and (34) are used to show the variation of drag with the location of the maximum section of a number of bodies whose forebody and afterbody profiles are parabolic arcs.

4.3. *Conical Bodies.*—The drag of forebodies or afterbodies whose geometry is the frustum of a cone is shown in Fig. 7. The slender body theory gives this drag as

$$C_D \,.\, a^2 = \frac{1}{b^4}\left[2(2b^2-2b+1)\log 2\beta - 2(b-1)^2\log\left(1-\frac{1}{b}\right)-1\right] \ldots \quad (35)$$

The notation is the same as in 4.2. With $b = 1$, (35) reduces to the first-order cone value:

$$C_D \,.\, a^2 = 2\log 2\beta - 1. \quad \ldots \quad (36)$$

Comparison with parabolic bodies (Fig. 7) shows that in general conical bodies have a considerably lower drag.

Fig. 8 shows the interference drag of some double-cone bodies, given by

$$C_{D\,A2} \,.\, a^2 = \frac{2}{c^2}\{-(1+c+p)^2\log(1+c+p)+(c+p)(2+c+p)\log(c+p)$$
$$+(1+2(1+c)p+p^2)\log(1+p)-(2+2c+p)p\log p - c$$
$$+2c\log[2\beta(1+p)]-2cU_1(\beta p)\}. \quad \ldots \quad (37)$$

It is clear from Fig. 8 that the interference drag of conical bodies is in general greater than that of parabolic bodies. The physical explanation of this is as follows. Interference drag may be considered to be due to the negative pressures which would exist on a parallel portion situated in the region of the afterbody, acting on the actual afterbody. Now the suction on a parallel portion behind a conical forebody is greater than that behind a parabolic one; and, furthermore, a conical afterbody has more projected area near its forward end, where the suction is greatest, than a parabolic afterbody. Both these effects lead to a higher interference drag. However, for low values of $c\beta = l_F/R_1\sqrt{(M^2-1)}(<2)$, equation (37) gives negative values of interference drag. This marks a definite collapse of the theory, for exact solutions for a cone ahead of a parallel portion always give a negative pressure coefficient immediately behind the shoulder, indicating positive interference drag.

We consider finally the interference drag of symmetrical, open-ended conical bodies; this is

$$C_{D\,A2} \,.\, a^2 = \frac{4}{b^4}\{(1-2b-b^2-2bp-\tfrac{1}{2}p^2)\log(2+p)-(1-2b-b^2-4bp-p^2)\log(1+p)$$
$$-(2bp+\tfrac{1}{2}p^2)\log p - \tfrac{1}{2} + b^2\log[2\beta(1+p)]-b^2U_1(\beta p)\}. \quad \ldots \quad (38)$$

The results of (38) will be compared in the following section with those of the quasi-cylinder theory.

4.4. *Some Comparisons of Quasi-cylinder and Slender-Body Theory.*—The quasi-cylinder solutions for parabolic and conical forebodies or afterbodies are respectively,

$$C_D \, . \, a^2 = \frac{8}{\beta^2}\left(\frac{m}{b}\right)^4 T\left(\frac{\beta}{m}\right), \qquad (39)$$

$\left[\text{where} \qquad T(z) = z^2 U_1(z) - U_3(z) \text{ and } U_3(z) = \int_0^z t^2 \, U(t) \, dt\right],$

and
$$C_D \, . \, a^2 = 4\left(\frac{m}{b}\right)^2 U_1\left(\frac{\beta}{m}\right). \qquad (40)$$

m is the ratio of mean to maximum radius $R/R_{\max}$. (39) has also been obtained by Owen (Ref. 5), and (40) by Warren (Ref. 6); both these authors, however, used mean radii different from those used here. Throughout this report we take the arithmetic mean of the initial and final radii, *i.e.*, we write

$$R = \tfrac{1}{2}(R_0 + R_1). \qquad (41)$$

(39) and (40) now become

$$C_D \, . \, a^2 = \frac{1}{2\beta^2}\left(\frac{2b^2 - 1}{b^3}\right)^4 T\left(\frac{2\beta b^2}{2b^2 - 1}\right), \qquad (42)$$

and
$$C_D \, . \, a^2 = \left(\frac{2b - 1}{b^2}\right)^2 U_1\left(\frac{2\beta b}{2b - 1}\right). \qquad (43)$$

These results are compared with those of the slender-body theory in Figs. 9 and 10. The remarkable agreement in the case of conical bodies may be partly explained by considering the pressure distributions given by (1) and (10). (1) gives

$$C_p = \frac{2}{Bab} \, U\left(\frac{x}{BR}\right),$$

and this is also the dominating term in (10), with R replaced by R_0. However, a comparison of the pressure distributions would not always show as good agreement as is seen in Fig. 10; some cancellation of differences occurs in the integration.

In the case of the parabola, profile curvature introduces marked differences and the two sets of values only agree over a rather narrower range, $S_0/S_1 > 0 \cdot 6$. It may be noted, however, that in this range the agreement persists for very low values of the parameter $\beta = l/R_1 \sqrt{(M^2 - 1)}$. It is also fortunate that in the range $4 < l/R_1 \sqrt{(M^2 - 1)} < 12$, in which we are most interested at present from the viewpoint of application, the agreement between the two approximations is quite good down to fairly small values of the area ratio.

The quasi-cylinder solution for the interference drag of symmetrical, open-ended, conical bodies is

$$C_{D\,A2} \, . \, a^2 = 4\left(\frac{m}{b}\right)^2 \left\{ 2U_1\left[\frac{\beta(1+p)}{m}\right] - U_1\left[\frac{\beta(2+p)}{m}\right] - U_1\left[\frac{\beta p}{m}\right]\right\}, \qquad (44)$$

and, introducing the mean radius defined by (41), we have

$$C_{D\,A2} \, . \, a^2 = \left(\frac{2b - 1}{b^2}\right)^2 \left\{ 2U_1\left[\frac{2\beta b(1+p)}{2b-1}\right] - U_1\left[\frac{2\beta b(2+p)}{2b-1}\right] - U_1\left[\frac{2\beta bp}{2b-1}\right]\right\}. \qquad (45)$$

The results of (38) and (45) are shown in Fig. 11. In all cases the difference between the two approximations is small with respect to the total drag of the body; and as the area ratio approaches unity, the two solutions tend to coincide.

5. *Conclusions.*—The following general conclusions may be drawn, but it must be remembered that they are valid only to the order of accuracy of the theory and for profiles of reasonably small slope.

(*a*) The (principal) drag of a pointed or open forebody (or afterbody) is less for a conical than for the corresponding parabolic body (or ogive) except for pointed bodies with $l/R_1\sqrt{(M^2 - 1)} \geqslant 9$.

(*b*) For a body whose parallel portion is shorter than its forebody, the interference drag can be appreciable : it is in general higher for a conical than for a parabolic body.

(*c*) Comparison of the quasi-cylinder and slender-body approximations has shown good agreement for bodies of area ratio $S_0/S_{\max} > 0 \cdot 6$, even where the fineness ratio was small. The slender-body theory may therefore be applied with some confidence to all bodies of small profile slope.

APPENDIX I

Special Functions

The function $U(z)$ is derived in Ref. 2. Its definition in terms of z is lengthy and will not be quoted here, but it is readily defined in operational form (Refs. 3 and 4) by

$$U(z) = \frac{K_0(p)}{K_1(p)}, \quad \ldots \quad (I.1)$$

where the K_n's are modified Bessel functions of the second kind, and p is the Heaviside operator such that

$$p^{-1} = \int_0^z ds.$$

The Heaviside unit function which strictly speaking should appear in the equations above, is omitted here for simplicity.

It is apparent from the equations for pressure coefficient and drag in the main text, (1), (3), (10), (15), that functions of the following form may also arise in the calculation of drag:

$$U_1(z) = \int_0^z U(s)\, ds \quad \ldots \quad (I.2)$$

$$U_2(z) = \int_0^z sU(s)\, ds \quad \ldots \quad (I.3)$$

$$U_3(z) = \int_0^z s^2U(s)\, ds. \quad \ldots \quad (I.4)$$

$U(z)$ is tabulated in Ref. 2 for $z = 0$ to 10, and $U_1(z)$ for $z = 0$ to 10 has been calculated by Warren and Gunn (Ref. 6) using numerical integration.

In the present paper $U_2(z)$ and $U_3(z)$ for $z = 0$ to 10 have been calculated by numerical integration, and values of the four functions for $z = 10$ to 20 have been calculated from the first three terms of their asymptotic expansions. The expansions were obtained in the following manner, which is similar to the method used by Ward (Ref. 4) to find the asymptotic expansion of $W(z) = - U'(z)$.

Expanding the right side (I.1) in ascending powers of p, we obtain

$$\frac{K_0(p)}{K_1(p)} = -p\log p + (\log 2 - \gamma)p + \tfrac{1}{2}p^3\log^2 p - \tfrac{1}{2}(1 - 2\gamma + 2\log 2)p^3\log p$$

$$+ \tfrac{1}{4}(2\gamma^2 - 2\gamma - 4\gamma\log 2 + 2\log^2 2 + 2\log 2 + 1)p^3 + \ldots\,, \quad .. \qquad \text{(I.5)}$$

where γ is Euler's constant. If we write the digamma function as $\Psi(\zeta)$ we have the standard forms

$$\Psi(\zeta) = \frac{d}{d\zeta}(\log \zeta!) = \lim_{n\to\infty}\left(\log n - \frac{1}{\zeta+1} - \frac{1}{\zeta+2}\cdots - \frac{1}{\zeta+n}\right),$$

and $\quad \gamma = -\Psi(0).$

To interpret (I.5) we apply the following operational laws. ζ is a complex variable and M is a contour consisting of a small circle about the origin and the upper and lower sides of a cut along the negative real axis.

$$p^n = \frac{1}{2\pi i}\int_M \zeta^{n-1}e^{z\zeta}\,d\zeta = \frac{1}{z^n.(-n)!}, \quad .. \quad .. \quad .. \quad .. \quad .. \qquad \text{(I.6a)}$$

$$= 0 \text{ for } n \text{ a positive integer.} \quad .. \quad .. \quad .. \quad .. \quad .. \quad .. \qquad \text{(I.6b)}$$

$$p^n\log p = \frac{1}{2\pi i}\int_M \zeta^{n-1}\log\zeta\, e^{z\zeta}\,d\zeta = \frac{1}{z^n.(-n)!}[\Psi(-n) - \log z] \quad .. \quad .. \qquad \text{(I.7a)}$$

$$= \frac{(-1)^n(n-1)!}{z^n} \text{ for } n \text{ a positive integer.} \quad .. \quad .. \quad .. \quad .. \qquad \text{(I.7b)}$$

$$p^n\log^2 p = \frac{1}{2\pi i}\int_M \zeta^{n-1}\log^2\zeta\, e^{z\zeta}\,d\zeta,$$

$$= \frac{1}{z^n.(-n)!}[\log^2 z - 2\log z\,\Psi(-n) + \Psi^2(-n) - \Psi'(-n)], \quad .. \qquad \text{(I.8a)}$$

$$= -2\log z\,\frac{(-1)^n(n-1)!}{z^n} + \frac{2(-1)^n(n-1)!}{z^n}\left[-\gamma + 1 + \tfrac{1}{2}\ldots + \frac{1}{n-1}\right]$$

for n a positive integer. .. .. (I.8b)

Applying these results to (I.5) we obtain

$$U(z) \sim \frac{1}{z} + \frac{1}{z^3}(2\log 2z - 2) + \ldots\,. \quad .. \quad .. \quad .. \quad .. \quad .. \qquad \text{(I.9)}$$

(I.9) could also have been obtained by writing

$$U(z) = \int_z^\infty W(s)\,ds,$$

and applying Ward's expansion for $W(z)$, but the following expansions could not be obtained in such a manner.

The operational form of $U_1(z)$ is $K_0(p)/pK_1(p)$ and so we obtain

$$U_1(z) \sim \log 2z + \frac{1}{2z^2}(1 - 2\log 2z) + \ldots\,. \quad .. \quad .. \quad .. \quad .. \qquad \text{(I.10)}$$

We now write, integrating (I.3) by parts,

$$U_2(z) = zU_1(z) - \int_0^z U_1(s)\, ds\,,$$

$$= zU_1(z) - \frac{K_0(p)}{p^2 K_1(p)}\,,$$

$$\sim z - \frac{2}{z} \log 2z + \ldots \qquad \text{(I.11)}$$

Also $$U_3(z) = z^2 U_1(z) - 2\int_0^z sU_1(s)\, ds\,. \qquad \text{(I.12)}$$

To obtain the operational form of $zU_1(z)$ we use the result that if $F(p) = f(z)$,

$$zf(z) = -p\frac{d}{dp}\left[\frac{F(p)}{p}\right],$$

so that (I.12) becomes

$$U_3(z) = z^2 U_1(z) + 2\frac{d}{dp}\left[\frac{K_0(p)}{p^2 K_1(p)}\right]. \qquad \text{(I.13)}$$

In evaluating the last term we obtain the correct result if we reverse the order of differentiation and expansion in series, but to justify this step is no simple matter. We therefore proceed as follows.

Since $K_0'(p) = -K_1(p)$ and $\frac{d}{dp}[pK_1(p)] = -pK_0(p)$,

$$\frac{d}{dp}\left[\frac{K_0(p)}{p.pK_1(p)}\right] = -\frac{1}{p^2} - \frac{K_0(p)}{p^3 K_1(p)} + \frac{1}{p^2}\left[\frac{K_0(p)}{K_1(p)}\right]^2.$$

We expand this by means of (I.5), and, interpreting (I.13), we finally obtain

$$U_3(z) \sim \frac{z^2}{2} - 2\log 2z + \log^2 2z - \Psi'(0), \qquad \text{(I.14)}$$

where $$\Psi'(0) = 1 + \tfrac{1}{4} + \tfrac{1}{9} \ldots = \frac{\pi^2}{6}. \qquad \text{(I.14)}$$

NOTATION

a = l/BR of a quasi-cylinder forebody (section 3.2) *also*, fineness ratio (length/maximum radius) of a fore- or afterbody, l_F/R_1 or l_A/R_1 (section 4)

a_i Values of x at which discontinuities in slope occur

b = l/BR of a quasi-cylinder forebody + parallel portion (section 3.2) *also*, ratio of length of the corresponding pointed body to length of a fore- or afterbody (section 4)

b_i Increase in slope at a discontinuity

B = $\sqrt{(M^2 - 1)}$

c	=	l/BR of a quasi-cylinder (sections 2.1, 3) *also*, ratio of forebody length to afterbody length l_F/l_A (section 4)
C_p		Pressure coefficient $(p - p_0)/\frac{1}{2}\rho_0 V_0^2$
C_D		Wave-drag coefficient based on $S_{\max}$
D		Wave drag
l		Length
m		Ratio of mean to maximum radius of a quasi-cylinder
M		Free-stream Mach number
p		Ratio of length of parallel portion to afterbody length l_p/l_A (section 4) *also*, Heaviside operator (Appendix I)
R		Mean radius of a quasi-cylinder
$R(x)$		Radius of slender body at any point
R_i		Radius of slender body at a point of discontinuity in slope, $R(a_i)$
$S(x)$		Cross-section area
t		Thickness ratio (maximum diameter/length)
$T(x)$		Function associated with $U(x)$ (section 4.4)
$U(x)$		Function derived and tabulated by Lighthill (Ref. 2 and Appendix I)
$\left.\begin{matrix} U_1(x) \\ U_2(x) \\ U_2(x) \end{matrix}\right\}$		Functions associated with $U(x)$ (Appendix I)
$W(x)$	=	$-U'(x)$
x		Axial co-ordinate measured from nose of body
z	=	x/BR for quasi-cylinder
β	=	a/B, i.e., $l_F/R_1\sqrt{(M^2-1)}$ or $l_A/R_1\sqrt{(M^2-1)}$ (section 4)
$\eta(z)$		Slope of quasi-cylinder dr/dx
Ψ		Digamma function
$(\ )_A$		Afterbody
$(\ )_F$		Forebody
$(\ )_{\max}$		Maximum cross-section (in general cases)
$(\ )_1$		Maximum cross-section (in some particular cases)
$(\ )_p$		Parallel portion
$(\ )'$		Differentiation

REFERENCES

No.	Author	Title, etc.
1	Th. von Kármán and N. B. Moore ..	Resistance of slender bodies moving with supersonic velocities, with special reference to projectiles. *Transactions of the A.S.M.E.*, Vol. 54. 1932.
2	M. J. Lighthill	Supersonic flow past bodies of revolution. R. & M. 2003. January, 1945.
3	M. J. Lighthill	Supersonic flow past slender bodies of revolution the slope of whose meridian section is discontinuous. *Quart. Jour. Mech. and Appl. Maths.*, Vol. 1, Part 1. March, 1948.
4	G. N. Ward	The approximate external and internal flow past a quasi-cylindrical tube moving at supersonic speeds. *Quart. Jour. Mech. and Appl. Maths.*, Vol. 1, Part 2. June, 1948.
5	P. R. Owen and R. G. Anderson ..	Unpublished work on intake drag at theRoyal Aircraft Establishment.
6	C. H. E. Warren and R. E. W. Gunn ..	Estimation of external drag of an axially symmetric conical nose entry for jet engine at supersonic speeds. R.A.E. Tech. Note Aero. 1934. A.R.C. 12,009. January, 1948.
7	G. N. Ward	Supersonic flow past slender pointed bodies. *Quart. Jour. Mech. and Appl. Maths.*, Vol. 2, Part 1. March, 1949.
8	L. E. Fraenkel	Supersonic flow past slender bodies of elliptic cross-section. R.A.E. Report Aero. 2466. 1952.

TABLE 1

Special Functions

$U(z) = K_0(p)/K_1(p)$.

$U_1(z) = \int_0^z U(s)\, ds,\ U_2(z) = \int_0^z sU(s)\, ds,\ U_2(z) = \int_0^z s^2U(s)\, ds.$

$T(z) = z^2U_1(z) - U_3(z)$.

Origin of tabulated values

$z = 0$ to 10 — $U(z)$ from Ref. 2. $U_1(z)$, $U_2(z)$ $U_3(z)$ by numerical integration, $U_1(z)$ being taken from Ref. 6.

$z = 10$ to 20 — First three terms of the functions' asymptotic expansions (Appendix I).

z	$U(z)$	$U_1(z)$	$U_2(z)$	$U_3(z)$	$T(z)$
0	1·00000	0	0	0	0
0·2	0·90703	0·1905	0·0187	0·0025	0·005
0·4	0·82646	0·3636	0·0704	0·0185	0·040
0·6	0·75621	0·5217	0·1492	0·0583	0·130
0·8	0·69462	0·6667	0·2505	0·1295	0·297
1·0	0·64034	0·8001	0·3703	0·2377	0·562
1·2	0·59229	0·9232	0·5056	0·3867	0·943
1·4	0·54960	1·0374	0·6538	0·5796	1·454
1·6	0·51149	1·1434	0·8127	0·8181	2·109
1·8	0·47737	1·2422	0·9806	1·1036	2·921
2·0	0·44672	1·3346	1·1560	1·4369	3·901
2·2	0·41907	1·4211	1·3376	1·8184	5·060
2·4	0·39408	1·5024	1·5244	2·2482	6·406
2·6	0·37140	1·5789	1·7156	2·7262	7·947
2·8	0·35080	1·6511	1·9104	3·2523	9·692
3·0	0·33201	1·7193	2·1082	3·8261	11·648
3·2	0·31483	1·7840	2·3086	4·4472	13·821
3·4	0·29909	1·8454	2·5111	5·1154	16·217
3·6	0·28464	1·9037	2·7152	5·8299	18·842
3·8	0·27134	1·9593	2·9208	6·5906	21·702
4·0	0·25906	2·0123	3·1275	7·3969	24·800
4·4	0·23721	2·1115	3·5436	9·144	31·73
4·8	0·21840	2·2025	3·9620	11·069	39·68
5·2	0·20209	2·2865	4·3819	13·169	48·66
5·6	0·18785	2·3644	4·8025	15·440	58·71
6·0	0·17534	2·4370	5·2232	17·880	69·85
6·4	0·16428	2·5049	5·6439	20·488	82·11
6·8	0·15445	2·5686	6·0642	23·262	95·51
7·2	0·14567	2·6286	6·4840	26·201	110·07
7·6	0·13778	2·6853	6·9031	29·303	125·80
8·0	0·13068	2·7389	7·3216	32·567	142·72
8·4	0·12424	2·7899	7·7394	35·992	160·86
8·8	0·11839	2·8384	8·1564	39·579	180·23

TABLE 1—*continued*

z	$U(z)$	$U_1(z)$	$U_2(z)$	$U_3(z)$	$T(z)$
9·2	0·11304	2·8847	8·5728	43·326	200·84
9·8	0·10815	2·9289	8·9883	47·232	222·70
10·0	0·10366	2·9712	9·4032	51·299	245·82
10·0	0·10399	2·971	9·401	51·36	245·7
10·5	0·09879	3·021	9·470	56·74	276·4
11·0	0·09405	3·070	10·438	62·25	309·2
11·5	0·08976	3·116	10·955	68·06	344·0
12·0	0·08586	3·159	11·470	74·12	380·8
12·5	0·08227	3·201	11·985	80·42	419·8
13·0	0·07898	3·242	12·499	86·97	460·9
13·5	0·07594	3·280	13·012	93·77	504·1
14·0	0·07313	3·318	13·524	100·81	547·5
14·5	0·07052	3·354	14·036	108·10	597·0
15·0	0·06809	3·388	14·547	115·64	646·7
15·5	0·06582	3·422	15·057	123·42	698·6
16·0	0·06370	3·454	15·567	131·46	752·8
16·5	0·06172	3·485	16·076	134·73	814·2
17·0	0·05985	3·516	16·585	148·26	867·8
17·5	0·05810	3·545	17·094	157·03	928·7
18·0	0·05644	3·574	17·602	166·05	991·9
18·5	0·05488	3·602	18·110	175·32	1057·4
19·0	0·05340	3·629	18·617	184·83	1125·2
19·5	0·05200	3·655	19·124	194·59	1195·3
20·0	0·05067	3·681	19·631	204·61	1267·7

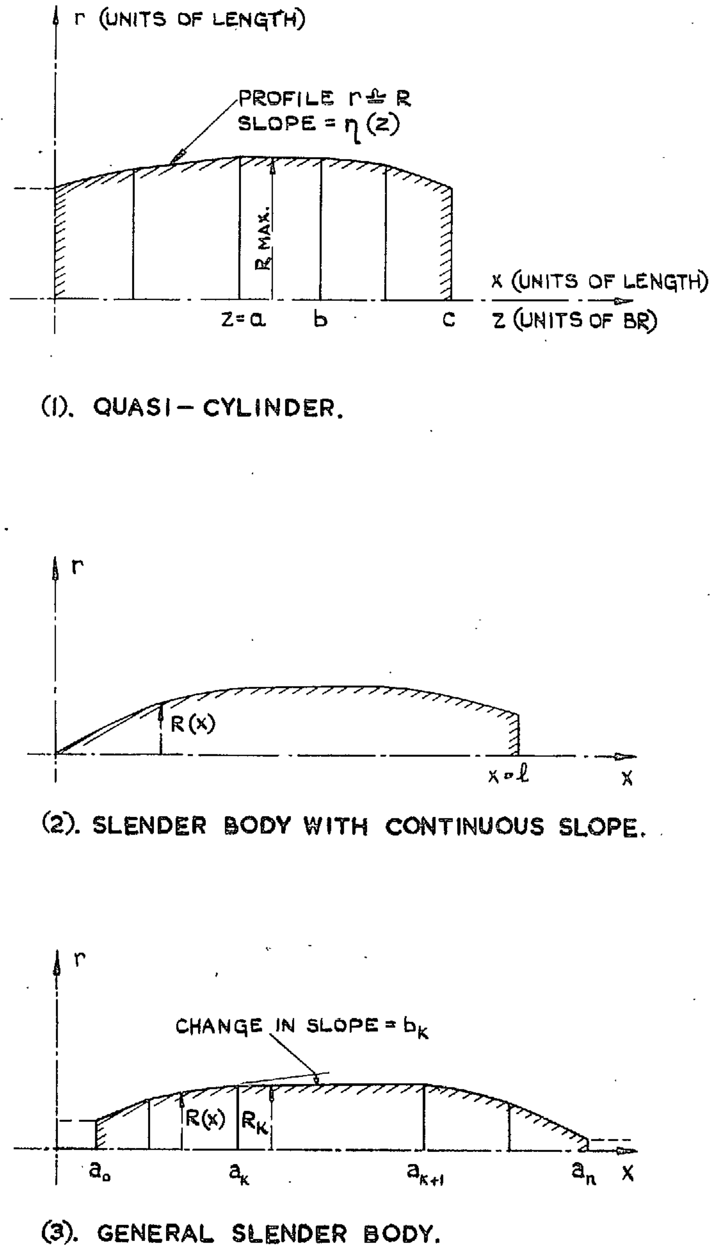

FIG. 1. Notation.

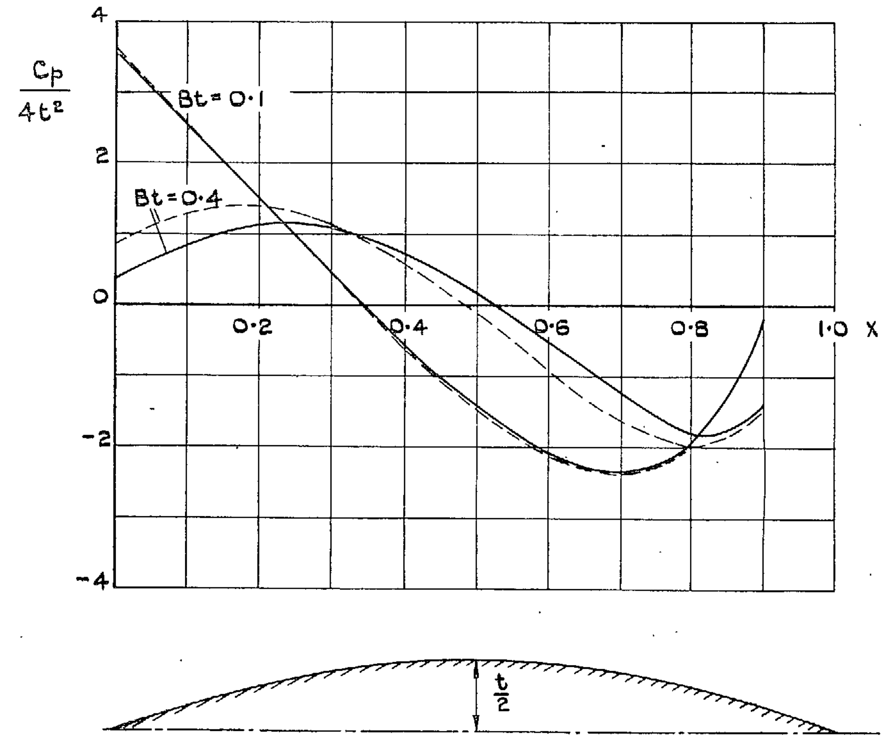

———— $C_p = \frac{1}{\pi}\int_0^{x-BR(x)} \frac{S''(y)}{\sqrt{(x-y)^2 - B^2R^2(x)}}\,dy - R'^2(x)$

- - - - - $C_p = \frac{1}{\pi}\int_{y=0-}^{x} \log \frac{2(x-y)}{BR(x)}\, dS''(y) - R'^2(x)$

FIG. 2. Pressure distribution for a pointed body of parabolic profile.

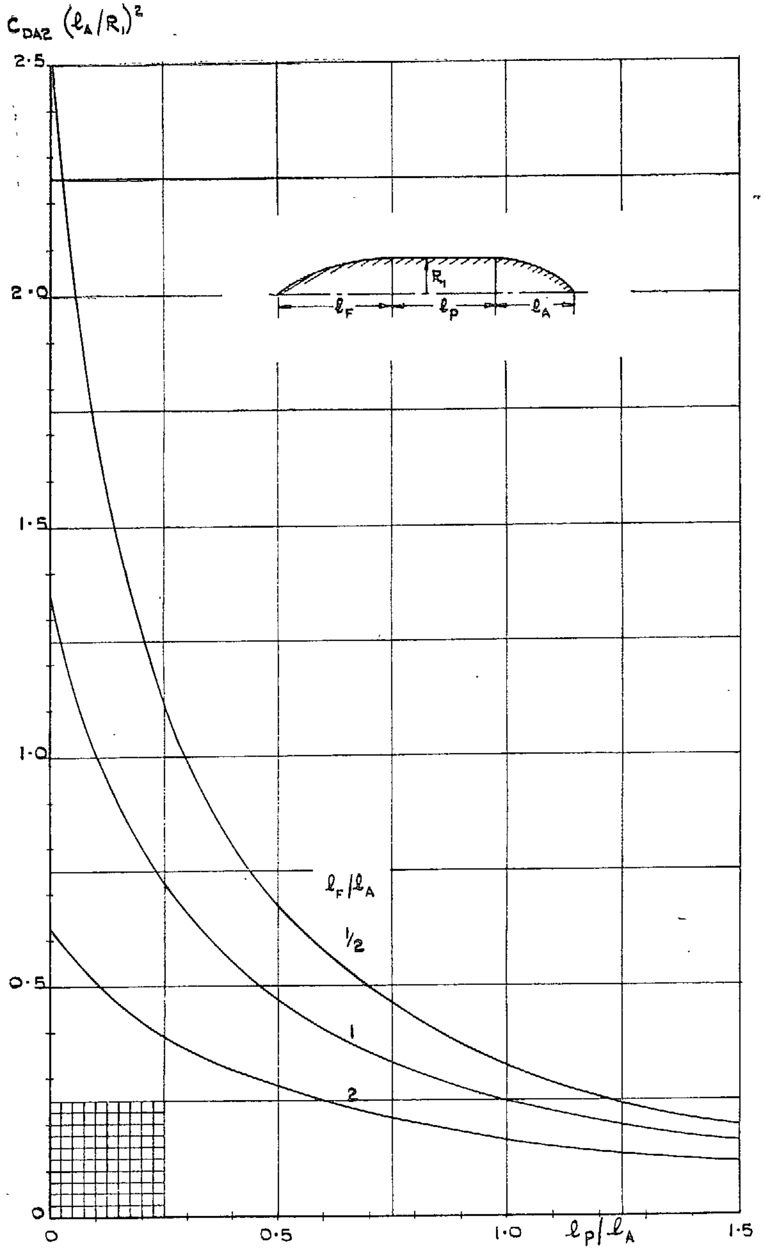

FIG. 4. Interference drag for pointed bodies of parabolic profile.

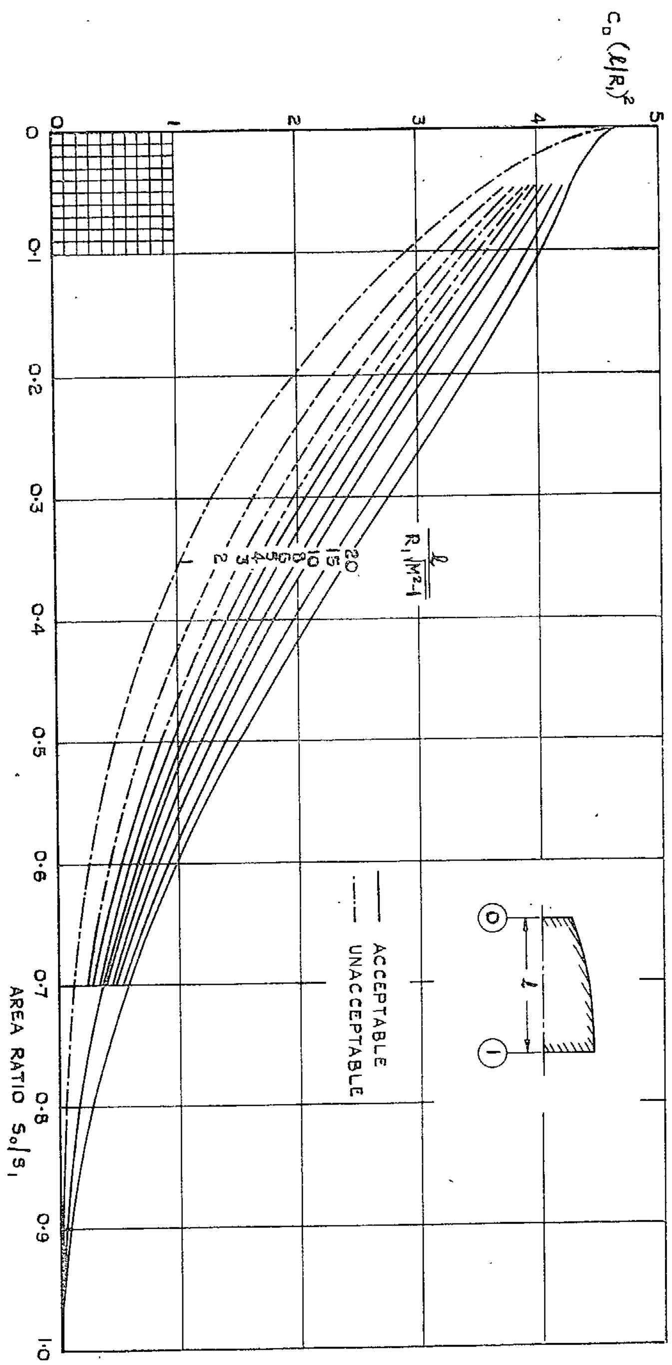

FIG. 3. Drag of (slender) fore- or afterbodies of parabolic profile.

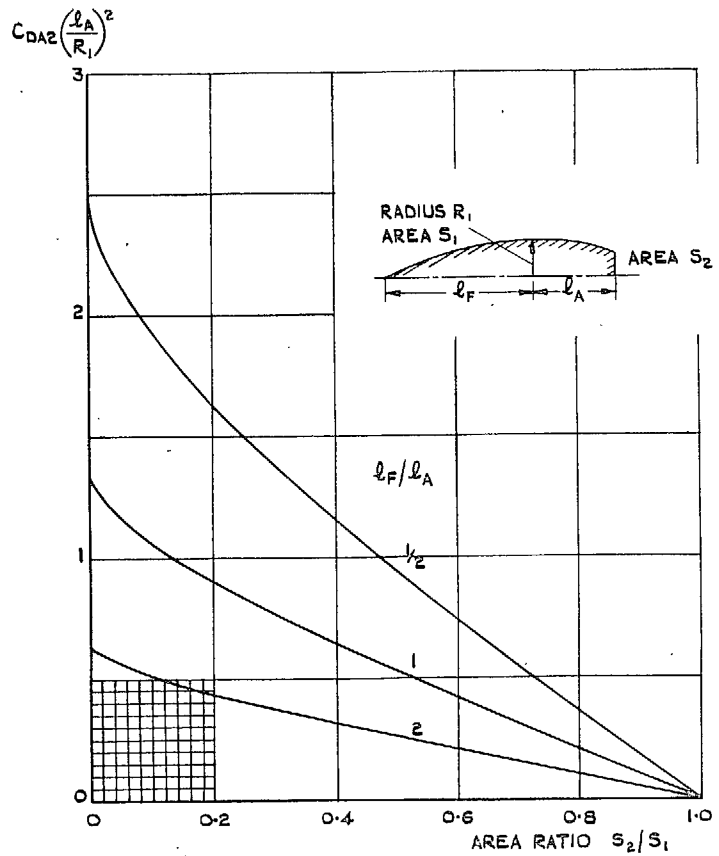

FIG. 5. Interference drag of truncated afterbodies behind pointed forebodies. (Parabolic profiles : no parallel portion.)

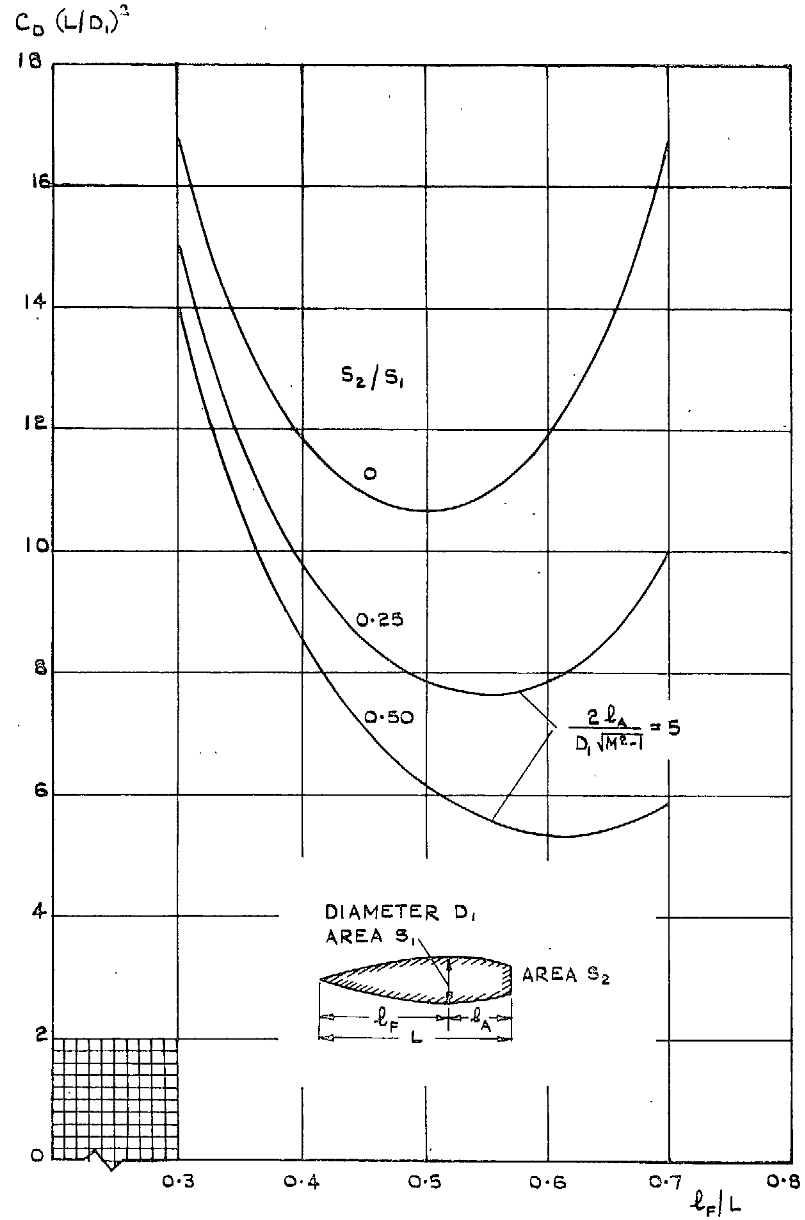

FIG. 6. Effect of maximum section location on body drag. (Parabolic profiles.)

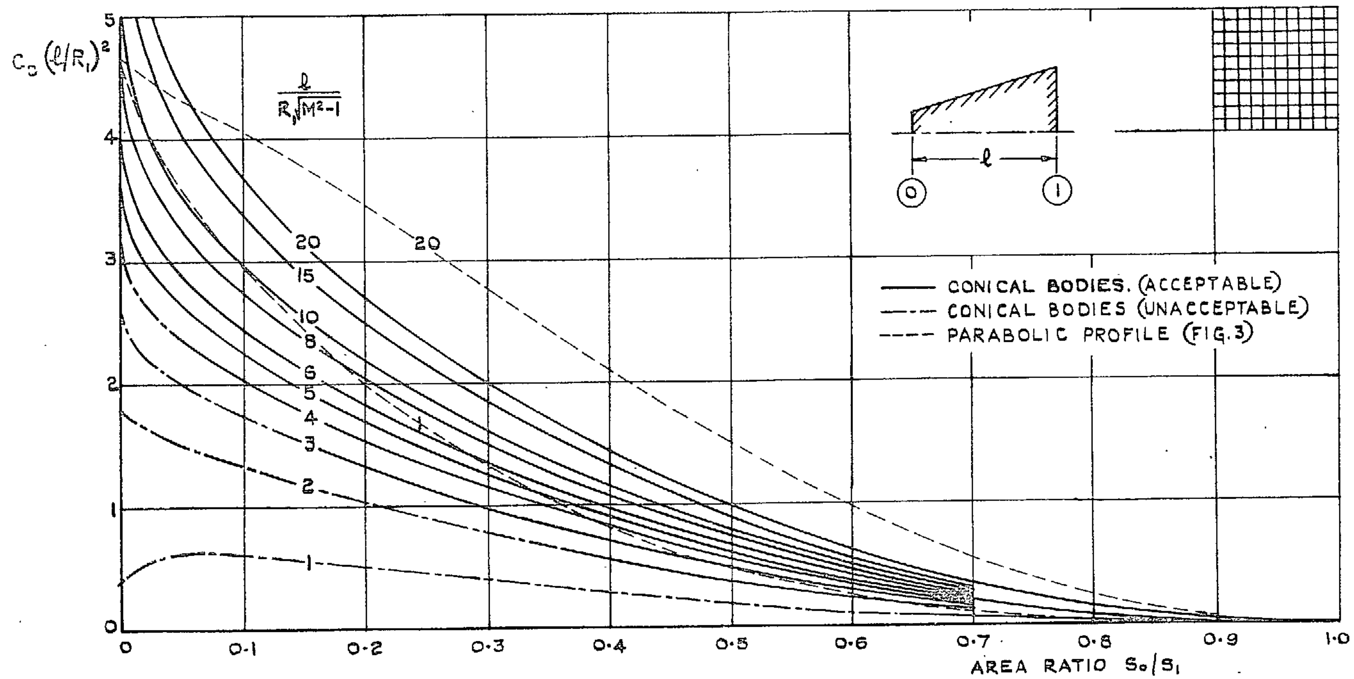

FIG. 7. Drag of (slender) conical fore- or afterbodies.

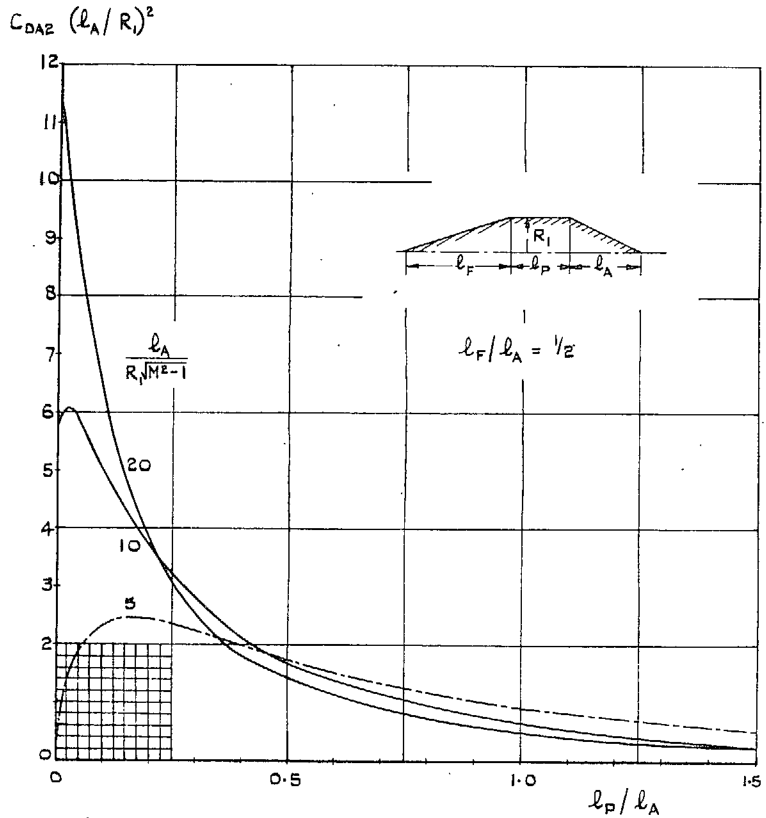

FIG. 8a. Interference drag of pointed conical bodies.

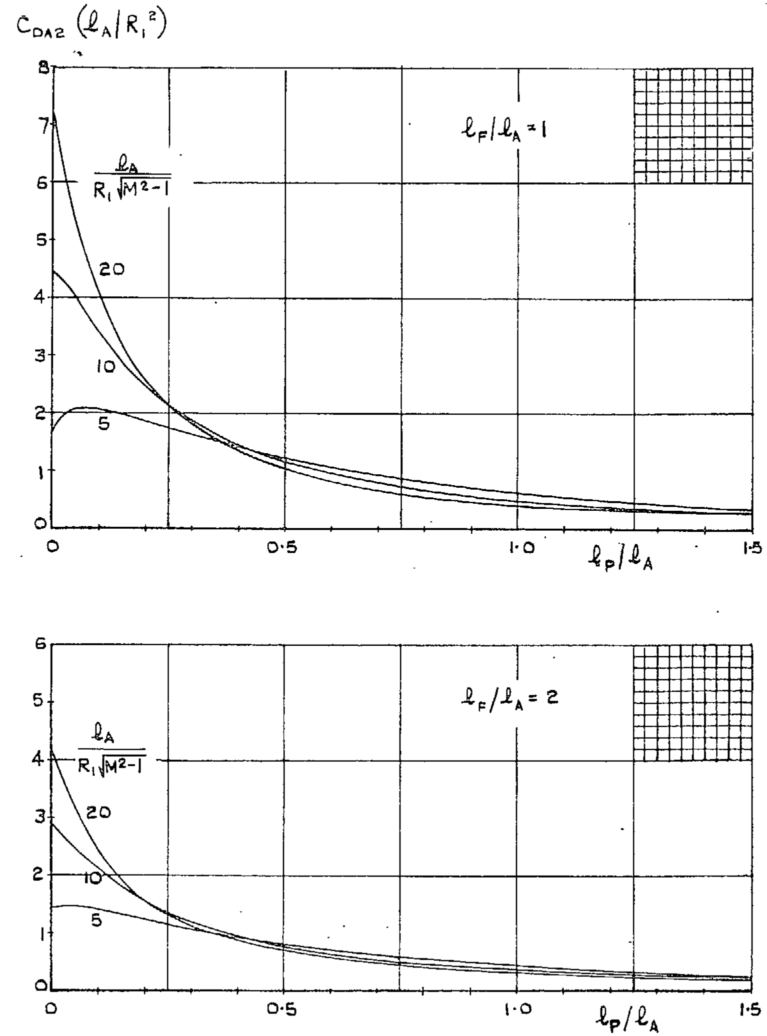

FIGS. 8b and 8c. Interference drag of pointed conical bodies.

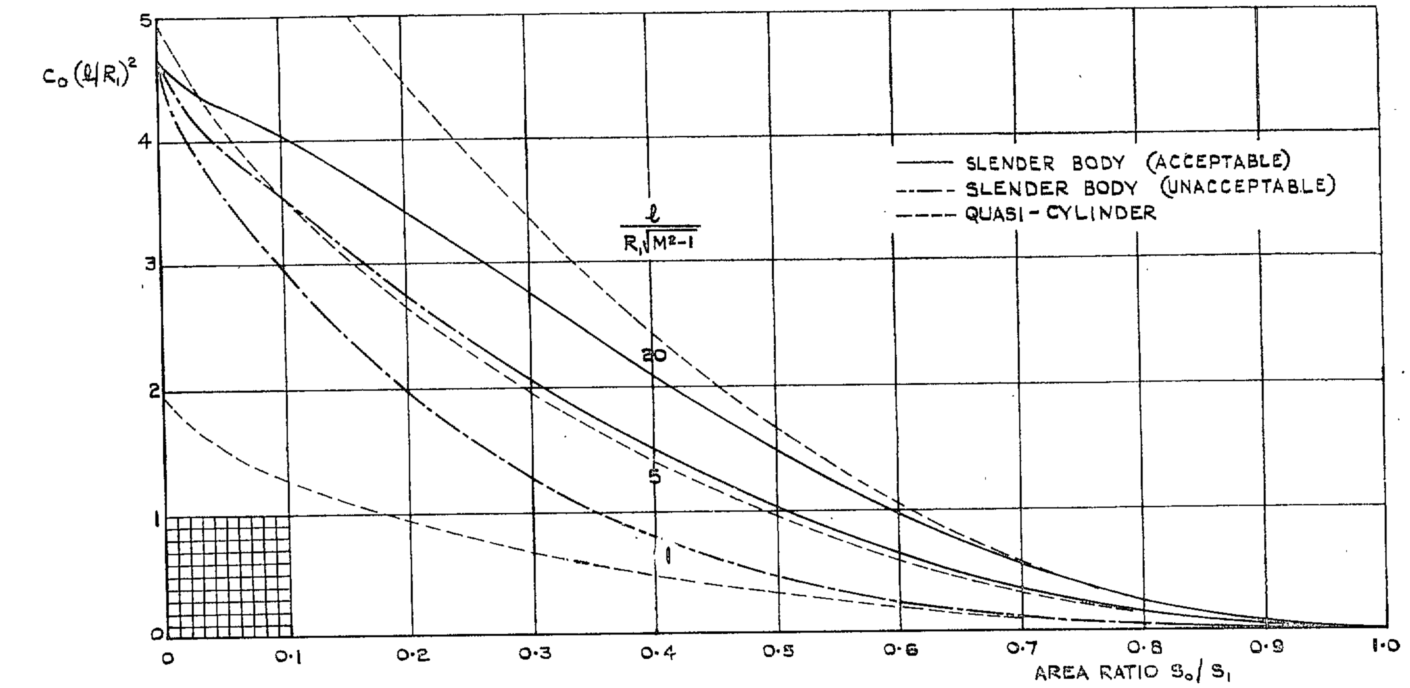

FIG. 9. Comparison of slender body and quasi-cylinder solutions for fore- or afterbodies of parabolic profile.

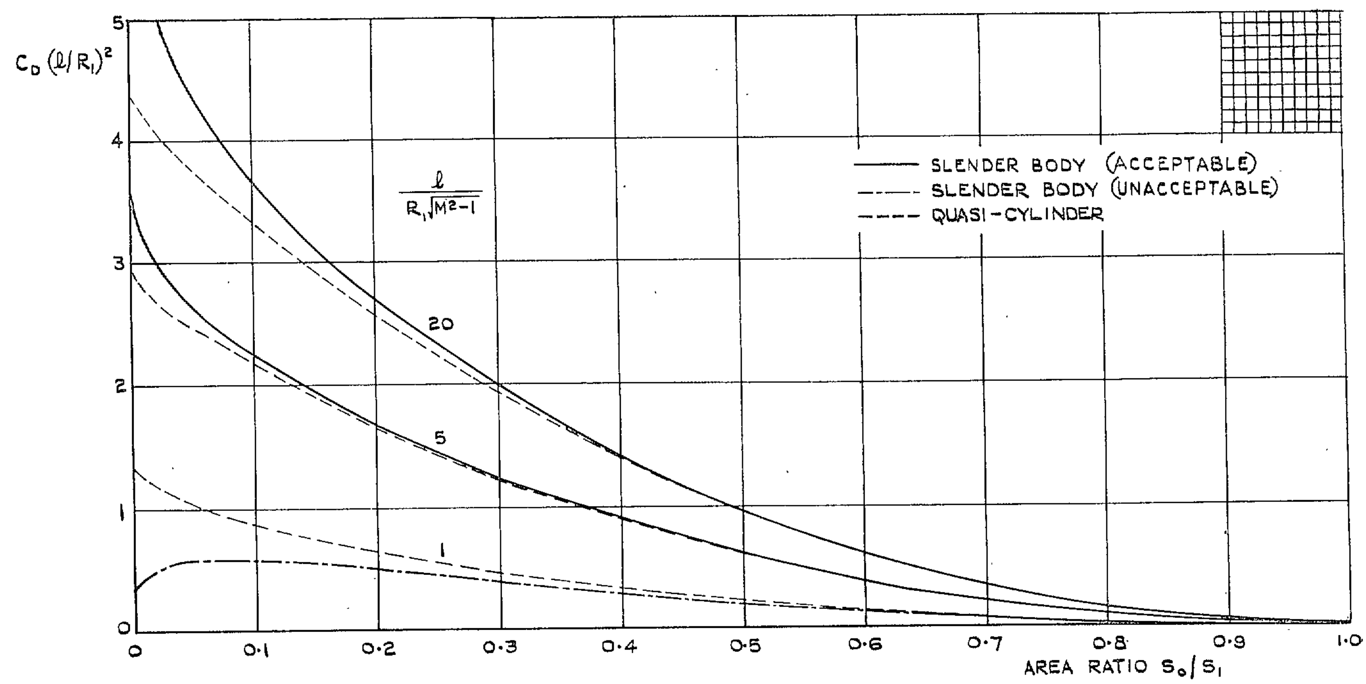

FIG. 10. Comparison of slender body and quasi-cylinder solutions for conical fore- or afterbodies.

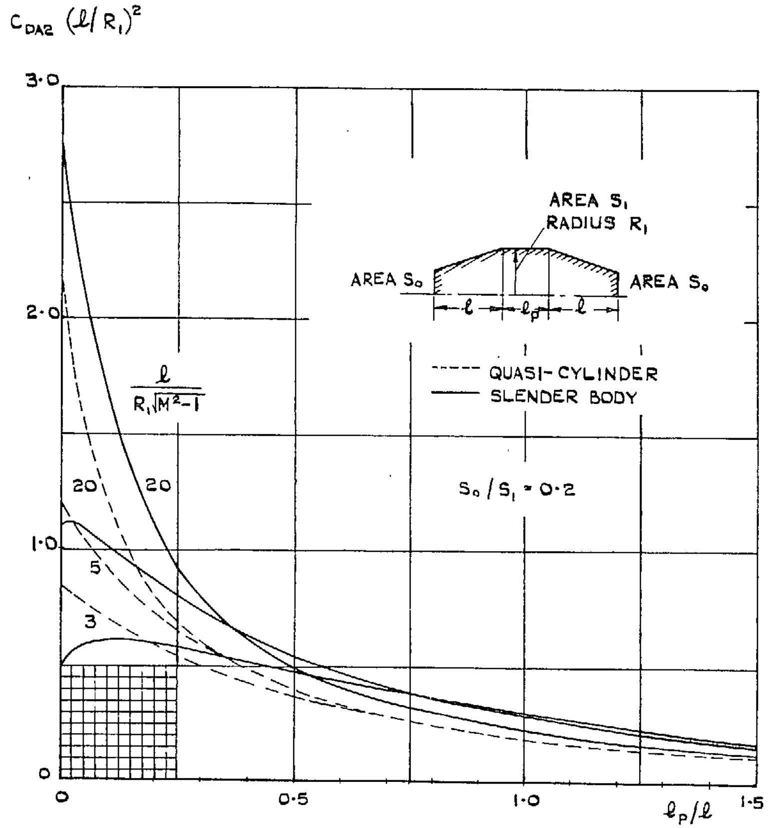

FIG. 11a. Interference drag of open-ended conical bodies (area ratio 0·2).

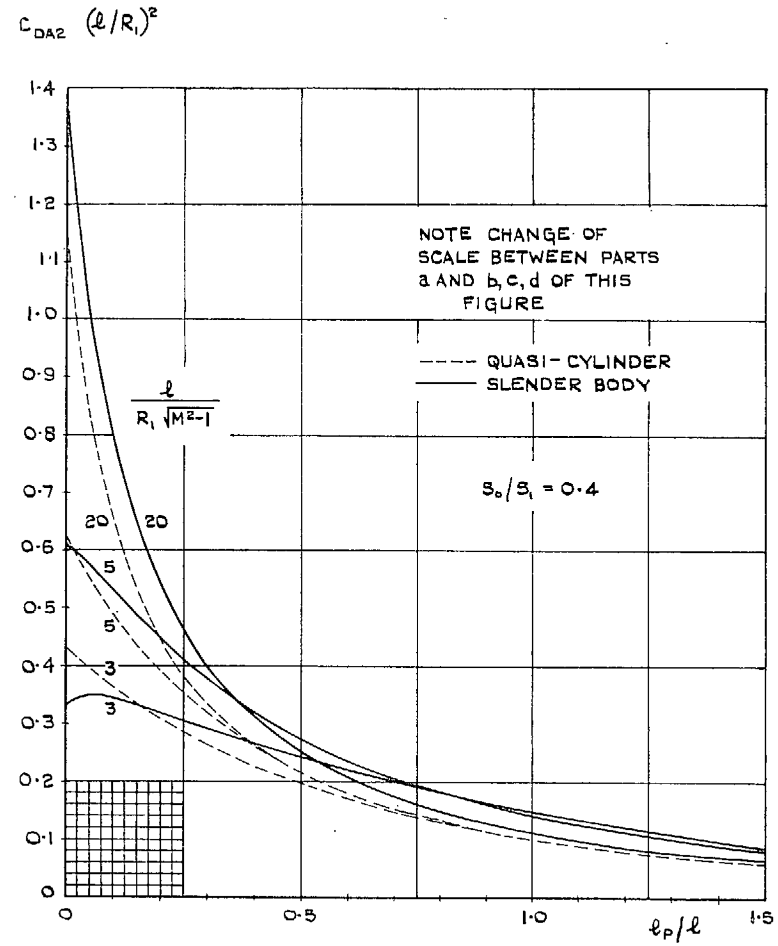

FIG. 11b. Interference drag of open-ended conical bodies (area ratio 0·4).

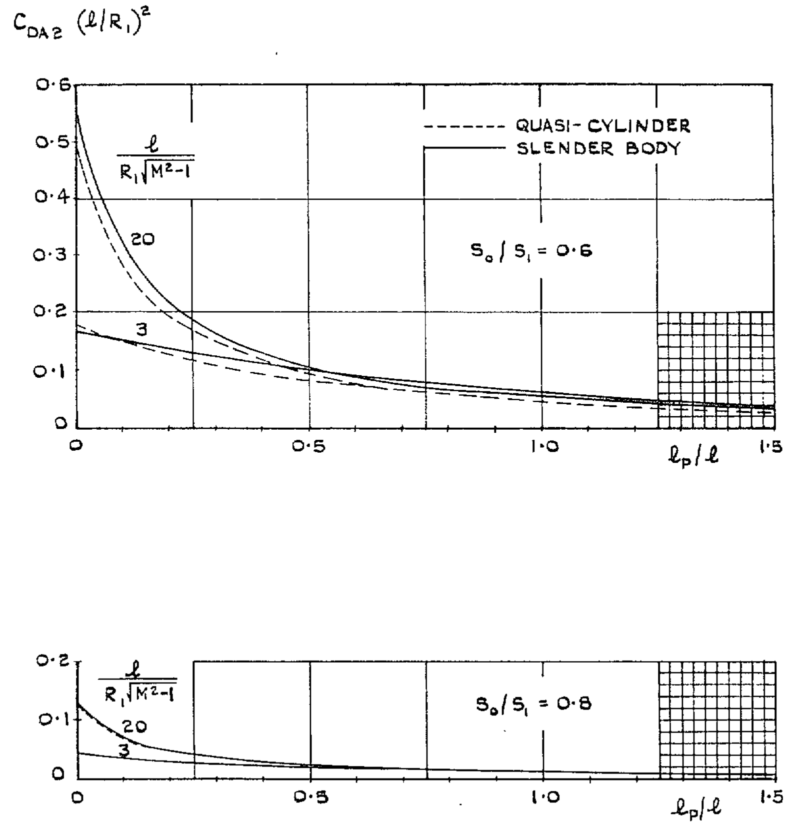

FIGS. 11c and 11d. Interference drag of open-ended conical bodies (area ratios 0·6 and 0·8).

J4314 Wt.18/9296 K9 6/55 D&Co. 34/263

PRINTED IN GREAT BRITAIN

Publications of the Aeronautical Research Council

ANNUAL TECHNICAL REPORTS OF THE AERONAUTICAL RESEARCH COUNCIL (BOUND VOLUMES)

1936 Vol. I. Aerodynamics General, Performance, Airscrews, Flutter and Spinning. 40s. (41s. 1d).
Vol. II. Stability and Control, Structures, Seaplanes, Engines, etc. 50s. (51s. 1d.)

1937 Vol. I. Aerodynamics General, Performance, Airscrews, Flutter and Spinning. 40s. (41s. 1d.)
Vol. II. Stability and Control, Structures, Seaplanes, Engines, etc. 60s. (61s. 1d.)

1938 Vol. I. Aerodynamics General, Performance, Airscrews. 50s. (51s. 1d.)
Vol. II. Stability and Control, Flutter, Structures, Seaplanes, Wind Tunnels, Materials. 30s. (31s. 1d.)

1939 Vol. I. Aerodynamics General, Performance, Airscrews, Engines. 50s. (51s. 1d.)
Vol. II. Stability and Control, Flutter and Vibration, Instruments, Structures, Seaplanes, etc. 63s. (64s. 2d.)

1940 Aero and Hydrodynamics, Aerofoils, Airscrews, Engines, Flutter, Icing, Stability and Control, Structures, and a miscellaneous section. 50s. (51s. 1d.)

1941 Aero and Hydrodynamics, Aerofoils, Airscrews, Engines, Flutter, Stability and Control, Structures. 63s. (64s. 2d.)

1942 Vol. I. Aero and Hydrodynamics, Aerofoils, Airscrews, Engines. 75s. (76s. 3d.)
Vol. II. Noise, Parachutes, Stability and Control, Structures, Vibration, Wind Tunnels. 47s. 6d. (48s. 7d.)

1943 Vol. I. Aerodynamics, Aerofoils, Airscrews, 80s. (81s. 4d.)
Vol. II. Engines, Flutter, Materials, Parachutes, Performance, Stability and Control, Structures. 90s. (91s. 6d.)

1944 Vol. I. Aero and Hydrodynamics, Aerofoils, Aircraft, Airscrews, Controls. 84s. (85s. 8d.)
Vol. II. Flutter and Vibration, Materials, Miscellaneous, Navigation, Parachutes, Performance, Plates, and Panels, Stability, Structures, Test Equipment, Wind Tunnels. 84s. (85s. 8d.)

ANNUAL REPORTS OF THE AERONAUTICAL RESEARCH COUNCIL—

1933–34	1s. 6d. (1s. 8d.)	1937	2s. (2s. 2d.)
1934–35	1s. 6d. (1s. 8d.)	1938	1s. 6d. (1s. 8d.)
April 1, 1935 to Dec. 31, 1936.	4s. (4s. 4d.)	1939–48	3s. (3s. 2d.)

INDEX TO ALL REPORTS AND MEMORANDA PUBLISHED IN THE ANNUAL TECHNICAL REPORTS, AND SEPARATELY—

April, 1950 - - - - - R. & M. No. 2600. 2s. 6d. (2s. 7½d.)

AUTHOR INDEX TO ALL REPORTS AND MEMORANDA OF THE AERONAUTICAL RESEARCH COUNCIL—

1909–1949 - - - - - - R. & M. No. 2570. 15s. (15s. 3d.)

INDEXES TO THE TECHNICAL REPORTS OF THE AERONAUTICAL RESEARCH COUNCIL—

December 1, 1936 — June 30, 1939.	R. & M. No. 1850.	1s. 3d. (1s. 4½d.)
July 1, 1939 — June 30, 1945.	R. & M. No. 1950.	1s. (1s. 1½d.)
July 1, 1945 — June 30, 1946.	R. & M. No. 2050.	1s. (1s. 1½d.)
July 1, 1946 — December 31, 1946.	R. & M. No. 2150.	1s. 3d. (1s. 4½d.)
January 1, 1947 — June 30, 1947.	R. & M. No. 2250.	1s. 3d. (1s. 4½d.)
July, 1951 - - - - -	R. & M. No. 2350.	1s. 9d. (1s. 10½d.)

Prices in brackets include postage.

Obtainable from

HER MAJESTY'S STATIONERY OFFICE

York House, Kingsway, London W.C.2 ; 423 Oxford Street, London W.1 (Post Orders : P.O. Box No. 569, London S.E.1) ; 13A Castle Street, Edinburgh 2 ; 39 King Street, Manchester 2 ; 2 Edmund Street, Birmingham 3 ; 109 St. Mary Street, Cardiff ; Tower Lane, Bristol 1 ; 80 Chichester Street, Belfast OR THROUGH ANY BOOKSELLER

S.O. Code No. 23-2842

R. & M. No. 2842